A peer-reviewed version of this preprint was published in PeerJ on 15 May 2019.

View the peer-reviewed version (peerj.com/articles/6881), which is the preferred citable publication unless you specifically need to cite this preprint.

Panagiotopoulou O, Pataky TC, Hutchinson JR. 2019. Foot pressure distribution in White Rhinoceroses (*Ceratotherium simum*) during walking. PeerJ 7:e6881 https://doi.org/10.7717/peerj.6881

Foot pressure distribution in White Rhinoceroses (*Ceratotherium simum*) during walking

Olga Panagiotopoulou Corresp., [1] , **Todd C Pataky** [2] , **John R Hutchinson** Corresp. [3]

[1] Monash Biomedicine Discovery Institute, Department of Anatomy and Developmental Biology, Moving Morphology & Functional Mechanics Laboratory, Monash University, Clayton, Victoria, Australia

[2] Department of Human Health Sciences, Kyoto University, Kyoto, Japan

[3] Department of Comparative Biomedical Sciences, Structure and Motion Laboratory, Royal Veterinary College, Hatfield, United Kingdom

Corresponding Authors: Olga Panagiotopoulou, John R Hutchinson
Email address: olga.panagiotopoulou@monash.edu, JHutchinson@rvc.ac.uk

White rhinoceroses (*Ceratotherium simum*) are odd-toed ungulates that belong to the group Perissodactyla and are second only to elephants in terms of large body mass amongst extant tetrapods, making them fascinating studies for how large land animals support and move themselves. Rhinoceroses often are kept in captivity for protection from ivory poachers and for educational/touristic purposes, yet a detrimental side effect of captivity can be foot disease (i.e. enthesopathies and osteoarthritis around the phalanges). Foot diseases in large mammals are multifactorial, but locomotor biomechanics (e.g. pressures routinely experienced by the feet) surely can be a contributing factor. However, due to a lack of *in vivo* experimental data on rhinoceros foot pressures, our knowledge of locomotor performance and its links to foot disease is limited. The overall aim of this study was to characterize peak pressures and centre of pressure trajectories in white rhinoceroses during walking. We asked two major questions. First, are peak locomotor pressures the lowest around the fat pad and its lobes (as in the case of elephants)? Second, are peak locomotor pressures concentrated around the areas with the highest reported incidence of pathologies? Our results show a reduction of pressures around the fat pad and its lobes, which is potentially due to the material properties of the fat pad or the fact that our rhinoceros subjects avoided “heel” contact at impact. We also found an even and gradual concentration of foot pressures across all digits, which may be a by-product of the more horizontal foot roll-off during the stance phase. While our exploratory, descriptive sample precluded hypothesis testing, our study provides important new data on rhinoceros locomotion for future studies to build on, and thus impetus for improved implementation in the care of captive/managed rhinoceroses.

Title: Foot pressure distribution in White Rhinoceroses (*Ceratotherium simum*) during walking.

Authors: Olga Panagiotopoulou[1], Todd C Pataky[2], John R Hutchinson[3]

1. Monash Biomedicine Discovery Institute, Department of Anatomy and Developmental Biology, Moving Morphology & Functional Mechanics Laboratory, Monash University, Victoria, Australia
2. Department of Human Health Sciences, Kyoto University, Kyoto, Japan
3. Department of Comparative Biomedical Sciences, Structure and Motion Laboratory, The Royal Veterinary College, Hatfield, UK

Corresponding authors:
Dr Olga Panagiotopoulou (olga.panagiotopoulou@monash.edu)
Professor John R Hutchinson (JHutchinson@rvc.ac.uk)

Abstract

White rhinoceroses (*Ceratotherium simum*) are odd-toed ungulates that belong to the group Perissodactyla and are second only to elephants in terms of large body mass amongst extant tetrapods, making them fascinating studies for how large land animals support and move themselves. Rhinoceroses often are kept in captivity for protection from ivory poachers and for educational/touristic purposes, yet a detrimental side effect of captivity can be foot disease (i.e. enthesopathies and osteoarthritis around the phalanges). Foot diseases in large mammals are multifactorial, but locomotor biomechanics (e.g. pressures routinely experienced by the feet) surely can be a contributing factor. However, due to a lack of *in vivo* experimental data on rhinoceros foot pressures, our knowledge of locomotor performance and its links to foot disease is limited. The overall aim of this study was to characterize peak pressures and centre of pressure trajectories in white rhinoceroses during walking. We asked two major questions. First, are peak locomotor pressures the lowest around the fat pad and its lobes (as in the case of elephants)? Second, are peak locomotor pressures concentrated around the areas with the highest reported incidence of pathologies? Our results show a reduction of pressures around the fat pad and its lobes, which is potentially due to the material properties of the fat pad or the fact that our rhinoceros subjects avoided "heel" contact at impact. We also found an even and gradual concentration of foot pressures across all digits, which may be a by-product of the more horizontal foot roll-off during the stance phase. While our exploratory, descriptive sample precluded hypothesis testing, our study provides important new data on rhinoceros locomotion for future studies to build on, and thus impetus for improved implementation in the care of captive/managed rhinoceroses.

Keywords: biomechanics, Perissodactyla, locomotion, osteopathology, mechanobiology, gait

Introduction

Over millions of years of evolution, the feet of rhinoceroses have had to change with other alterations of limb morphology, locomotor behaviour, body size, habitat and more (e.g. Prothero, 2005; Stilson et al., 2016). Extant rhinoceroses include the second largest (after elephants) extant terrestrial mammals, with body masses in the White rhinoceros reaching up to 3600 kg (Groves 1972; Hiilman-Smith et al., 1986; Owen-Smith 1992), so in large rhinoceroses locomotor stresses might be considerable if not well-controlled, imposing severe biomechanical constraints on form and function (Alexander and Pond, 1992). Contrary to feet of elephants, which bear five functional digits and "predigits" (Hutchinson et al., 2011; Mariappa, 1986; Neuville, 1935; Weissengruber et al., 2006), rhinoceros feet have three digits (numbered II-IV) terminating in horns/hooves (Prothero, 2005; Regnault et al., 2013) and no supportive "predigits". Of the three digits, digit II and IV respectively dominate the medial and lateral aspects of the foot, whilst digit III is the central and largest of all. Each digit consists of three phalanges (proximal, medial and distal) and the foot caudally and centrally is enclosed in a fat pat. The bilobed fat pad is structurally similar but smaller in size to elephant fat pads and expands when compressed (von Houwald 2001). This structure potentially helps to evenly distribute locomotor stresses across the sole of the foot, as in the case of elephants (Panagiotopoulou et al., 2012, 2016). Overall, the morphology of rhinoceros feet is fairly symmetrical from medial to lateral; unlike the feet of elephants which are more robust laterally (e.g. digits III-V).

Considering that large mammals' feet support their body mass during gait, understanding healthy foot function is important for understanding healthy gait. This is particularly important in view of documented rhinoceros foot pathologies (Dudley et al., 2014; Flach et al., 2003; Galateanu et al., 2013; Harrison et al., 2011; Jacobsen, 2002; Jones 1979; Regnault et al., 2013; Von Houwold 2001; Von Houwald and Guldenschuh 2002; Von Houwold and Flach, 1998; Zainuddin et al., 1990). Previous research on museum specimens found a high occurrence of enthesopathies and osteoarthritis on the phalanges of rhinoceros feet (Regnault et al., 2013)-- of the 81 feet from 27 rhinoceroses studied, 54 feet from 22 individuals exhibited osteopathologies (Dudley et al., 2014). Surprisingly, limb osteopathologies have remained remarkably common in rhinocerotid species across their evolution but increasing with estimated body mass, consistent

with tradeoffs and compromises between large size, cursorial/medioportal morphology or athletic capacity, and limb health (Stilson et al., 2016).

Many factors can cause foot disease in large mammals, but previous research in elephants has linked foot disease with obesity, space limitations and the time the animals spent walking or standing on hard (unnatural) surfaces (Csuti et al., 2001; Fowler and Mikota 2006; Miller et al., 2016). Our prior studies proposed that elephants normally have high pressures laterally, on digits III-V (Panagiotopoulou et al., 2012, 2016), congruent with where elephants tend to exhibit greater incidences of osteopathologies (Regnault et al., 2017). In contrast, there are almost no *in vivo* studies of locomotion in rhinoceroses (e.g. Alexander and Pond, 1992), in any aspects including the pressures experienced by the feet. Based on the roughly equivalent occurrence of osteopathologies across rhinoceros digits II-IV (Regnault et al., 2017), we expect that pressures would be evenly distributed across these digits too, and for pressures to be low on the fat pad lobes; without the mediolateral asymmetry of pathologies or pressures observed in elephant feet.

In this pilot study, we describe *in vivo* locomotor foot pressures and centre of pressure trajectories (COP) in three white rhinoceroses (*Ceratotherium simum*) during walking. Our limited sample size does not allow us to conduct hypothesis testing on foot pressure magnitudes. However, we were able to conduct preliminary, qualitative evaluation of our two hypotheses, for future studies to expand on:

Hypothesis I. Peak locomotor pressures will be the lowest in the central and caudal parts of the foot at the locations of the fat pad and its lobes. This is expected from a dynamic interaction of behavioural walking preferences (manifested in COP) and the compliant properties of the fat pad, as we have previously observed in elephants (Panagiotopoulou et al., 2012, 2016).

Hypothesis II. Peak locomotor pressures will be concentrated equally around the horns/hooves and phalangeal pads of all digits (II-IV), which correspond to the overlying bony areas with the highest evidence of osteoarthritis and similar pathologies (Regnault et al, 2013); without a strong tendency for more lateral prevalence of pathology.

Methods

Subjects

Two adults and a juvenile captive southern White Rhinoceros (*Ceratotherium simum*) from Colchester Zoo (Colchester, UK) participated in the study (Table 1). The body masses of the subjects were estimated by the zoo keepers using the zoo's records. Zoo keepers and veterinarians gave clinical consent for the study and all animal participants were healthy. The study was approved by The Royal Veterinary College's Animal Ethics Committee (approval number URN 2010 1052).

Data collection

A 5m walkway was constructed in a crush area in the rhinoceros enclosure (Figure 1A). A 3m long and 0.4m wide foam pad was laid at the beginning of the walkway and was followed by a 1.0 x 0.4m pressure plate (fitted with 8192 sensors, 2.05 sensors cm^{-2}) (Footscan; RSscan, Olen, Belgium), and a 1m length of foam pad. The walkway was covered with a 0.3mm thick rubber mat to prevent the animals from recognising the location of the pressure plate. Reflective tape was placed on the rhinoceros hip and shoulder to calculate walking speeds using a Sony HDR (Sony, London, UK) high definition video camera. The camera was placed perpendicular to and at a 2m distance from the walkway. Camera and pressure plate sampling frequencies were respectively 25Hz and 250Hz. The pressure plate was calibrated using a known weight (~95kg human standing on the plate) as per manufacturer's instructions. While we do report absolute pressure magnitudes, the main outcome of interest was the relative (i.e. within-foot) pressure distribution, as this reflects foot functionality. Absolute pressure errors are unexpected to affect relative pressure values. The rhinoceros were guided over the walkway using food as encouragement, an average of 20 times each.

Trials with obvious acceleration and deceleration (as judged by video) during data collection were excluded from further analysis (Panagiotopoulou et al., 2012, 2016). Animal discomfort was kept to the minimum by stopping data collection when animals appeared disengaged.

Data processing

Data analysis protocols were similar to Panagiotopoulou et al., (2012, 2016), implanted in Canopy v. 2.1.8 using SciPy v. 0.19, NumPy 1.11.3 and Matplotlib 2.0 (Enthought Inc., Austin, TX, USA). In brief, the raw pressure data (x,y,time) of the individual footsteps were exported from the Footscan system, isolated algorithmically using spatio-temporal gaps between clusters of non-zero pressure voxels and were assessed for spatial and temporal completeness as per Panagiotopoulou et al., (2012, 2016). Individual images representative of spatio-temporally complete footsteps were manually identified as fore/hind, right/left; spatially scaled by a factor of 1.5, using bilinear interpolation to compensate for the non-square measurement grid of the RSscan system (7.62 x 5.08 mm, manufacturer specified) and spatially registered within subjects and feet (see Panagiotopoulou et al., (2012)). Following scaling and registration, nine anatomically homologous regions of interest (ROIs) were selected on the mean images for each foot as per Panagiotopoulou et al., (2012, 2016), and peak pressures (N cm^{-2}) of the whole stance phase were extracted from a three-pixel radius using a Gaussian kernel mean window with a standard deviation of one pixel. ROIs 1-3 respectively represented the horns of digits II-IV, ROIs 4-6 represented the (inter)phalangeal pads of digits II-IV respectively, ROI 7 represented the caudal most ("heel") aspect of the sole and ROIs 8-9 were respectively placed on the medial and lateral footpads of the sole (Figure 1B). Centre of pressure trajectories (COP) were computed as the pressure-weighted image centroids' time series after thresholding the images at 5 kPa. Due to the limited number of subjects and steps, the dependent variables were not tested for significance. This was a preliminary, qualitative study of rhinoceros foot function during gait, so we neither derived nor tested a null hypothesis.

Results

The mean walking speed of all three subjects was 0.53ms^{-1} (Table 1), which corresponded to a mean Froude number (Alexander & Jayes 1983; Fr = $velocity^2$ * [9.81 ms^{-2} * shoulder height]$^{-1}$) of 0.013, consistent with a slow walk. The peak pressure data per ROI, subject and feet are shown in Table 1. All peak pressure data are in Supplementary Data 1. The mean peak pressure values for the adult subjects 1 and 3 and all feet were respectively 220 kPa and 180 kPa, whilst the mean peak pressure values of the juvenile subject 2 were 9 kPa. The mean peak pressure values for both adult subjects and all feet (200kPa) were respectively 4.7 and 2.8 times lower than those previously recorded on African (946 kPa) and Asian elephants (567 kPa) during walking (Panagiotopoulou et al., 2012, 2016). The Asian elephant data were collected using the same RSscan system as in this study, yet the African elephant pressure data were collected using a lower resolution system (Zebris Medical GmbH, Biomechanix, Munich) with 100 Hz sampling frequency, 14,080 sensors in total and approximately 0.55 sensors cm^{-2}. Our data showed that, similar to elephants and other quadrupeds, the forefeet had higher mean pressure magnitudes than the hindfeet for all subjects (Table 1).

Contrary to elephants (Panagiotopoulou et al., 2012, 2016), the rhinoceroses' foot pressures did not follow a consistent pattern between feet. The forefeet for adult subject 2 and the juvenile rhino (subject 2) showed higher pressures around the horn of digits II (ROI 1), III (ROI 2) and IV (ROI 3). Intermediate pressures were recorded around the phalangeal pads of digits II-IV and the lowest pressures around the fad pad (ROIs 7-9) (Figures 2 & 3). The highest median foot pressures for the right forefeet of all three rhinoceroses were at the horn of digits III and IV, corresponding to ROIs 2 and 3 (Figures 2 & 4). The lowest median peak pressures were recorded around the fat pad; nevertheless, median peak pressures around the phalangeal pads of all digits were very low. Median pressures for the left hindfeet were the highest for the horn of digit II, followed by ROIs 2 & 3 (Figures 2 & 4). Intermediate median pressures were recorded at ROIs 4, 5 & 7 and the lowest peak pressures were computed at ROI 8. Regardless, median peak pressure differences

between ROIs 2-9 were minimal (Figure 2 & Supplementary Data 1.) Median peak pressures for the hindfeet of the two adult subjects (subject 1 & 3) gave the highest median peak pressures at the horn of digit II (ROI 1) and intermediate pressures at ROIs 2-4 (Figures 2 & 6). The lowest peak pressures were found at ROIs 5-9.

The COP trajectories for all time frames, animal participants and feet are shown in supplementary Figures S1- S8. Most COP traces began at the medial aspect of the foot caudally to the interphalangeal pad of digit II or at the medial footpad of the sole, then shifted caudally around the heel aspect of the sole and finally passed cranially through digit III by toe-off. Contrary to this caudo-medial and centrally-focused pressure pattern, pressure traces in two trials for the hind leftfoot started laterally on digit IV before shifting caudo-cranially and through digit III by toe-off. Thus there was some unusual variability in our subjects' COP traces during normal locomotion.

Discussion

Overall, we found reduction of peak pressures around the fat pad, qualitatively supporting our hypothesis I that, like in elephants, rhinoceros fat pads may keep locomotor pressures low due to their compliance. Whilst our quantitative results showed variation in peak foot pressures across feet, we recorded the highest peak pressures around the horn and phalangeal pads of all digits, yet this signal was not as strong for the left hindfoot (Figure 2). Such variations may be due to the ROI method used for data analysis. Although the ROI approach is a widely used technique for the estimation of peak pressure magnitudes sampled from specific anatomical regions, it overlooks variability within regions, assuming that all regions are functionally independent. We have previously shown a significant interaction between the topology of the ROIs and pressure magnitudes in elephants (Panagiotopoulou et al., 2016). Variation in peak pressures between ROIs may also have a biological importance considering that the left hindfoot sometimes showed a lateral-caudal-central roll off pattern, but we remain conservative with any biological conclusions due to our experimental and sample size limitations.

The general COP trajectories in our rhinoceros subjects were similar to elephants in being linear during the final half of stance phase rather than sigmoidal as in humans (Lord et al., 1986) and bonobos (Vereecke et al., 2003). However, contrary to elephants, our rhinoceros subjects loaded the medial part of the foot at impact and then shifted their load centrally during mid-stance prior to toe-off via their central digit. Reasons for this apparent preference to avoid "heelstrike", and the strongly medially-biased COP pattern in our subjects early in stance phase, remain unclear; but the variability of COP patterns is cause for caution in attributing this pattern to all rhinoceroses until more such data can be obtained and compared. Hints at other unusual COP patterns – or perhaps subject variability or measurement error – in large mammals (e.g. hippopotamus and tapir COP traces in Figure 1 of Michilsens et al., 2009) are further cause for caution and future analyses.

Due to this variation in rhinoceroses' foot pressures and COP trajectories, locomotor patterns are important for assessing peak pressure distributions qualitatively. The peak pressure "heat maps" for all subjects and steps shown in Figures 3-6 indicated a clear concentration of peak pressures around the horn and phalangeal pads of all three digits. These results tentatively support our hypothesis II-- that peak pressures are evenly distributed, rather than biased toward the central and lateral digits, which corresponds to the relatively even distribution of osteopathologies across digits II-IV (Regnault et al., 2013). An even distribution of peak pressures across all three digits might be a by-product of the horizontal position of the foot at impact as manifested by the COP traces (i.e. avoidance of heelstrike). Regardless, large animals such as elephants and rhinoceroses clearly use enlarged foot contact areas to protect the digits from peak pressures that otherwise could cause tissue damage (Chi and Roth, 2010; Michilsens et al., 2009).

It is also interesting that forefoot pressures were normally higher in our three subjects, and forefoot osteopathologies tend to be more common than hindfoot osteopathologies (Regnault et al., 2013)—although one study found more chronic foot disease overall in the hindfeet, rather than forefeet, of a sample of One-horned rhinoceroses (von Houwald and Flach, 1998). The latter study posited some biomechanical factors that may underlie foot pathologies, including toe horn-cracking, shearing forces on the middle toe, low friction causing low wear and overgrowth of the middle toe horn, which could inspire future studies building on this one. Regardless, these patterns are opposite those tentatively identified for elephants sampled by Regnault et al. (2017) — they found no clear forefoot vs. hindfoot differences in osteopathologies despite some evidence for higher pressures on elephant forefeet (Panagiotopoulou et al., 2012, 2016). It is tempting to speculate that the more similar morphology and presumably function of all four rhinoceros feet compared with the disparate morphology of elephant fore- vs. hindfeet may explain these discrepancies, but such speculations demand cautious future analysis.

Many factors account for osteopathologies such as congenital, developmental, metabolic, diet, age, traumatic injuries (summarised in Galateanu et al., 2013). However, captivity in enclosures with limited space for the animals to remain athletic, and exposure to hard concrete for long hours may exacerbate foot disease even if not the primary cause. To better understand foot pressures in rhinoceroses and the links to foot disease, more *in vivo* locomotor data are required; ideally from multiple species and management regimes.

Contrary to elephants that can easily be trained to walk over a walkway lined with pressure plates using food as encouragement, rhinoceroses are seldom well-trained, so *in vivo* data collection is challenging. We initially collected data on five animals but only a limited number of trials from this study's three individuals could be used for final analyses due to spatial (i.e. partial foot contacts) and temporal (i.e. starting data collection after initial foot contact and/or terminating data collection before final foot contact) completeness issues. We conducted a power analysis for a one-way ANOVA on our rhinoceros peak pressure data for each foot, where omega-squared was used for the effect size, significance was set at 0.01 and power was set at 0.8. The minimum number of rhinoceroses to achieve this power would be 8, 39, 29 and 13 for the left forefoot, right forefoot, left hindfoot and right hindfoot datasets respectively. Considering accessibility and experimental limitations, it will be difficult (if not impossible) to recruit enough rhinoceroses (>40 considering that some subjects would need to be discarded from any study) from the same captive setting for a statistically robust experiment.

Habitat loss and poaching have brought many rhinoceros species, in particular the Javan and the Sumatran, to the brink of extinction (Crosta et al., 2017). Despite on-going legal and conservation efforts to protect rhinoceroses, the number of populations impacted by poaching has increased dramatically over the last two decades, with South Africa being affected the most due to having the largest number of rhinoceroses in the world (Charlton 2017; Crosta et al., 2017). One of the measures in place to protect these animals from extinction is to keep and breed them in captivity. While in captivity, they may develop foot disorders, in particular chronic foot diseases, osteoarthritis, bone remodelling, osteitis-osteomyelitis, pododermatitis, abscesses, and fractures (Galateanu et al., 2013; Jacobsen 2002; Regnault et al., 2013; von Houwald & Flach 1998) that compromise animal welfare or even cause mortality due to being painful, progressive and often untreatable. Even in wild rhinoceroses, there are reports of serious foot disease (Zainuddin et al., 1990), and a high incidence of osteopathology appears to be an ancestral evolutionary trait for the lineage, which may complicate efforts to improve the welfare of rhinoceroses (Stilson et al., 2016). To date, most focus on appendicular pathologies in extant rhinoceroses have been on the feet, but the latter study's finding that pathologies have been equally prevalent across the limbs throughout the ~50 million year history of Rhinocerotidae raises questions of whether more proximal limb pathologies remain common but overlooked in captive rhinoceroses. Follow-up studies should investigate this question and

even integrate it with biomechanical analyses to test whether some regional mechanical stresses are unusually high in proximal elements and corresponding with locations predisposed to pathologies. Pond and Alexander (1992) used a very simple analysis to estimate that femur stresses and safety factors were high in galloping White rhinoceroses but this method certainly is imprecise, and stresses in humerus or zeugopodial elements are unknown--- as are any joint contact stresses, which should be more important for pathologies.

Disease management in large mammals such as elephants and rhinoceroses can be challenging and examination using diagnostic approaches requires general anaesthesia or sedation, which can have negative effects on the animal (Gage 2006; Hittmair & Vielgrader 2000; Siegal-Willott et al., 2012; von Houward & Flach 1998). These challenges, coupled with the fact that foot diseases may only clearly manifest themselves when they have progressed to advanced stages, can make euthanasia an unavoidable outcome (e.g. Jones 1979; Mikota 1999; Mikota et al., 1994). The causes of foot pathologies are multifactorial (e.g. Csuti et al., 2001), but the biomechanical pressures imposed during locomotion presumably can promote or worsen them. How can we thus protect rhinoceroses from developing foot diseases, or monitor treatment vs. progression of chronic foot disease? An important step is to learn how rhinoceros feet function in captivity. A valuable follow-on step would be to examine how husbandry conditions in captivity affect innate foot function. Nevertheless, whilst we have a fair understanding of elephant foot pressures from captive and semi-wild settings (Panagiotopoulou et al., 2012; 2016), here we have added new data on the pressures that White rhinoceroses routinely apply to their feet during normal locomotion, and these give tentative insights into not only basic biomechanics but also potential links of normal form and function vs. mechanically-induced foot disease.

Acknowledgements

We thank the keepers and members of staff at the Colchester Zoo, UK for their assistance with the experiments. We also thank RVC graduates Katherine Jones, Richard Harvey and Keri Holmes for assistance with data collection. Thanks are due to Hyab Mehari Abraha from Monash University and the Monash Bioinformatics Platform for technical support. This project was supported by Biotechnology and Biological Sciences Research Council (UK) grant number BB/H002782/1 to J.R.H.

Figure 1. A. Image of Subject 3 walking on the pressure plate in the experimental walkway. B. Schematic representation of the anatomical location of the nine regions of interest (ROI) across the left and right fore- and hindfeet.

Figure 2. Scatter plot of peak foot pressure data from all three subjects at the nine regions of interest (ROI) across the left forefoot, right forefoot, left hindfoot and right hindfoot respectively. Black line represents the median pressure found at each ROI.

Table 1. Subject characteristics (*Ceratotherium simum*).

Figure 3. Peak pressure patterns during the whole stance phase of the left forefoot of all subjects.

Figure 4. Peak pressure patterns during the whole stance phase of the right forefoot of all subjects.

Figure 5. Peak pressure patterns during the whole stance phase of the left hindfoot of all subjects.

Figure 6. Peak pressure patterns during the whole stance phase of the right hindfoot of all subjects.

Supplementary Data 1: Regional peak pressure data for all subjects and feet. Columns A-J show respectively the file name (A), subject ID (B), foot ID (C: left forefoot = 1; right forefoot = 2; left hindfoot = 3; right hindfoot = 4); ROI (D; also see Figure 1); peak pressure data in N cm^{-2} (E); walking speed in m s^{-1} (F); Shoulder height in metres (G); Froude number (H); Age (I; Adult=1; juvenile=2); Body mass estimate in kg (J; 1 = 2500; 2 = 1000). Some trials were excluded from further analyses due to being temporally incomplete. These are: [FORE LEFT: subject 1, trial 028_img001], [FORE RIGHT: subject 3, trial 033_img004; subject 3, trial 035_img003], HIND LEFT: subject 3, trial 010_img003], [HIND RIGHT: subject 3, trial 041_img006; subject 1, trial 001_img002; subject 1, trial 013_img005].

Supplementary Figure S1: Image time series of the COP trajectories (light grey) for the left forefoot of subject 1 (010_img002 [A] and 027_img002 [B]).

Supplementary Figure S2: Image time series of the COP trajectories (light grey) for the left forefoot of subject 2 (trials 018_img005 [A], 021_img005 [B] and 031_img002 [C]).

Supplementary Figure S3: Image time series of the COP trajectories (light grey) for the right forefoot of subject 1 (trials 27_10_035_img002 [A] and 27_10_img002 [B]).

Supplementary Figure S4: Image time series of the COP trajectories (light grey) for the right forefoot of subject 2 (trials 004_img007 [A], 009_img006 [B], 011_img004 [C] and 033_img003 [D]).

Supplementary Figure S5: Image time series of the COP trajectories (light grey) for the left hindfoot of subject 1 (trials 27_10_038_img005 [A] and 014_img002 [B]).

Supplementary Figure S6: Image time series of the COP trajectories (light grey) for the left hindfoot of subject 2 (trial 026_img004).

Supplementary Figure S7: Image time series of the COP trajectories (light grey) for the left hindfoot of subject 3 (trial 034_img003).

Supplementary Figure S8: Image time series of the COP trajectories (light grey) for the right hindfoot of subject 1 (trials 27_10_037_img003 [A] and 032_img003 [B]) and subject 2 (trial 27_10_019_img001 [C]).

References

Alexander RM, Pond CM. 1992. Locomotion and bone strength of the white rhinoceros, *Ceratotherium simum*. Journal of Zoology 227(1): 63-69

Alexander RMN, Jayes AS. 1983. A dynamic similarity hypothesis for the gaits of quadrupedal mammals. Journal of Zoology 201: 135–152 (doi:10.1111/j.1469-7998.1983.tb04266.x)

Charlton RW. 2017. Death and destruction: insight into the rhino poaching epidemic in South Africa. Illinois State University. *Theses and Dissertations*. 661. https://ir.library.illinoisstate.edu/etd/661

Chi KJ, Roth VL. 2010. Scaling and mechanics of carnivoran footpads reveal the principles of footpad design. Journal of the Royal Society Interface 7(49): 1145-1155

Crosta A, Sutherland K, Talerico C. 2017. Grinding rhino: An undercover investigation on rhino horn trafficking in China and Vietnam. Elephant Action League Report

Csuti B, Sargent EL, Bechert US. 2001. *The elephant's foot: prevention and care of foot conditions in captive Asian and African elephants*. Ames, IA: Iowa State University Press.

Dudley RJ, Wood SP, Hutchinson JR, Weller R. 2014. Radiographic protocol and normal anatomy of the hind feet in the white rhinoceros (*Ceratotherium simum*). Veterinary Radiology & Ultrasound 56 (2): 124-132 (doi.org/10.1111/vru.12215)

Flach E, Walsh T, Dodds J, White A, Crowe O. 2003. Treatment of osteomyelitis in a greater one-horned rhinoceros (*Rhinoceros unicornis*). Verh.Erkrg. Zootiere 41: 1–7

Fowler ME, Mikota SK. 2006. *Biology, medicine, and surgery of elephants*. Ames, IA: Blackwell Publishing Ltd.

Gage L. 2006. *Radiology*. In: Fowler ME, Mikota SK, editors. Biology, Medicine, and Surgery of Elephants. Ames, IA: Blackwell Publishing. pp. 192–197

Galateanu G, Hildebrandt TB, Maillot A, Etienne P, Potier R, Mulot B, Saragusty J, Hermes R. 2013. One small step for rhinos, one giant leap for wildlife management- imaging diagnosis of bone pathology in distal limb. Plos One 8(7): e68493 (doi: 10.1371/journal.pone.0068493)

Groves CP. 1972. *Ceratotherium simum*. Mammalian species 8: 1-6.

Harrison T, Stanley B, Sikarskie J, Bohart G, Ames N, Tomlian J, Marquardt M, Marcum A, Kiupel M, Sledge D, Agnew D. 2011. Surgical amputation of a digit and vacuum-assisted-closure (V.A.C.) management in a case of osteomyelitis and wound care in an eastern black rhinoceros (*Diceros bicornis michaeli*). Journal of Zoo and Wildlife Medicine 42: 317–321

374 Hillman-Smith, AKK, Owen-Smith N, Anderson JL, Hall-Martin AJ, Selaladi JP. 1986. Age estimation of
375 the white rhinoceros (*Ceratotherium simum*). Journal of Zoology 210 (3): 355-377 (doi: 10.1111/j.1469-
376 7998.1986.tb03639.x)
377
378 Hittmair KM, Vielgrader HD. 2000. Radiographic diagnosis of lameness in African elephants (*Loxodonta*
379 *africana*). Veterinary Radiology & Ultrasound 41 (6):511-515
380
381 Hutchinson JR, Delmer C, Miller CE, Hildebrandt T, Pitsillides AA, Boyde AJ. 2011. From flat foot to fat
382 foot: the structure, ontogeny, function and evolution of elephant 'sixth toes'. Science 344: 1699–1703
383 (doi:10.1126/science.1211437)
384
385 Jacobsen J. 2002. *A Review of Rhino Foot Problems*. In: Proc. 2nd Rhino Keepers' Workshop 2001.
386 Zoological Society of San Diego, San Diego, California. Pp. 56–59.
387
388 Jones D. 1979. The husbandry and veterinary care of captive rhinoceroses. International Zoo Yearbook
389 19: 239–250
390
391 Lord M, Reynolds DP, Hughes JR. 1986. Foot pressure measurement: a review of clinical findings. Journal
392 of Biomedical Engineering 8: 283-294.
393
394 Mariappa D. 1986. Anatomy and histology of the Indian elephant. Oak Park, MI: Indira Publishing House.
395
396 Michilsens F, Aerts P, Van Damme R, D'Août K. 2009. Scaling of plantar pressures in mammals. Journal
397 of Zoology 279(3): 236-242.
398
399 Mikota SK, Sargent EL, Ranglack GS. 1994. *Medical Management of the Elephant*. Indira Publishing
400 House, West Bloomfield, Michigan.
401
402 Mikota SK. 1999. *Diseases of the elephant: a review*. In Erkrankungen der Zootiere: Verhandlungsbericht
403 des 39. Internationalen Symposiums uber die Erkrankungen der Zoo undWildtiere, pp. 1–15.
404
405 Miller MA, Hogan JN, Meehan CL. 2016 Housing and demographic risk factors impacting foot and
406 musculoskeletal health in African elephants (*Loxodonta africana*) and Asian elephants (*Elephas maximus*)
407 in North American Zoo. PLoS ONE 11, e0155223. (doi:10.1371/journal.pone.0155223)

Neuville H. 1935. Sur quelques caractères anatomiques du pied des éléphants. Arch Mus Natl d'Histoire Naturelle, Paris, 6 e Série 13: 111–183

Owen-Smith RN. 1992. *Megaherbivores: the influence of very large body size on ecology*. Cambridge university press.

Panagiotopoulou O, Pataky TC, Day M, Hensman MC, Hensman S, Hutchinson JR, Clemente CJ. 2016. Foot pressure distributions during walking in African elephants (*Loxodonta africana*). Royal Society Open Science 3:160203 (http://dx.doi.org/10.1098/rsos.160203)

Panagiotopoulou O, Pataky TC, Hill Z, Hutchinson JR. 2012. Statistical parametric mapping of the regional distribution and ontogenetic scaling of foot pressures during walking in Asian elephants (*Elephas maximus*). Journal of Experimental Biology 215: 1584–1593 (doi:10.1242/jeb.065862)

Prothero DR. 2005. *Evolution of North American Rhinoceroses*. Cambridge University Press

Regnault S, Dixon JJI, Warren-Smith C, Hutchinson JR, Weller R. 2017. Skeletal pathology and variable anatomy in elephant feet assessed using computed tomography. PeerJ 5:e2877 (doi:10.7717/peerj.2877)

Regnault S, Hermes R, Hildebrandt T, Hutchinson J, Weller R. 2013. Osteopathology in the feet of rhinoceroses: lesion type and distribution. Journal of Zoo and Wildlife Medicine 44: 918–927 (doi: 10.1638/2012-0277R1.1 PMID: 24450050)

Siegal-Willott JL, Alexander A, Isaza R. 2012. *Digital Radiography of the Elephant Foot*. In: Fowler ME, Miller RE, editors. Zoo and Wild Animal Medicine, Current Therapy. St. Louis, Missouri: Elsevier Saunders. pp. 515–523

Stilson KT, Hopkins SSB, Davis EB. 2016. Osteopathology in Rhinocerotidae from 50 Million Years to the Present. PLoS ONE 11(2): e0146221 (doi:10.1371/journal.pone.0146221)

von Houwald F, Flach EJ. 1998. Prevalence of chronic foot disease in captive greater one-horned rhinoceros (*Rhinoceros unicornis*). EAZWV Sci. Meet 2: 323-327.

von Houwald F, Guldenschuh G. 2002. *Husbandry manual for the greater one-horned or Indian rhinoceros (Rhinoceros unicornis*) Linne, 1758. Basel Zoo, Basel, Switzerland.

von Houwald F. 2001. Foot problems in Indian rhinoceroses (*Rhinoceros unicornis*) in zoological gardens: macroscopic and microscopic anatomy, pathology,and evaluation of the causes. Ph.D. dissertation, Univ. of Zurich, Zurich, Switzerland

Weissengruber GE, Egger GF, Hutchinson JR, Groenewald HB, Elsasser L, Famini D, Forstenpointner G. 2006. The structure of the cushions in the feet of African elephants (*Loxodonta africana*). Journal of Anatomy 209: 781–792 (doi:10.1111/j. 1469-7580.2006.00648.x)

Zainuddin ZZ, Abdullah MT, Shamsuddin M, Suri M. 1990. The husbandry and veterinary care of captive Sumatran rhinoceros at Zoo Melaka, Malaysia. Malayan Nature Journal (Malaysia).

Figure 1

A. Image of Subject 3 walking on the pressure plate in the experimental walkway. B. Schematic representation of the anatomical location of the nine regions of interest (ROI) across the left and right fore- and hindfeet

A. Image of Subject 3 walking on the pressure plate in the experimental walkaway. B. Schematic representation of the anatomical location of the nine regions of interest (ROI) across the left and right fore- and hindfeet.

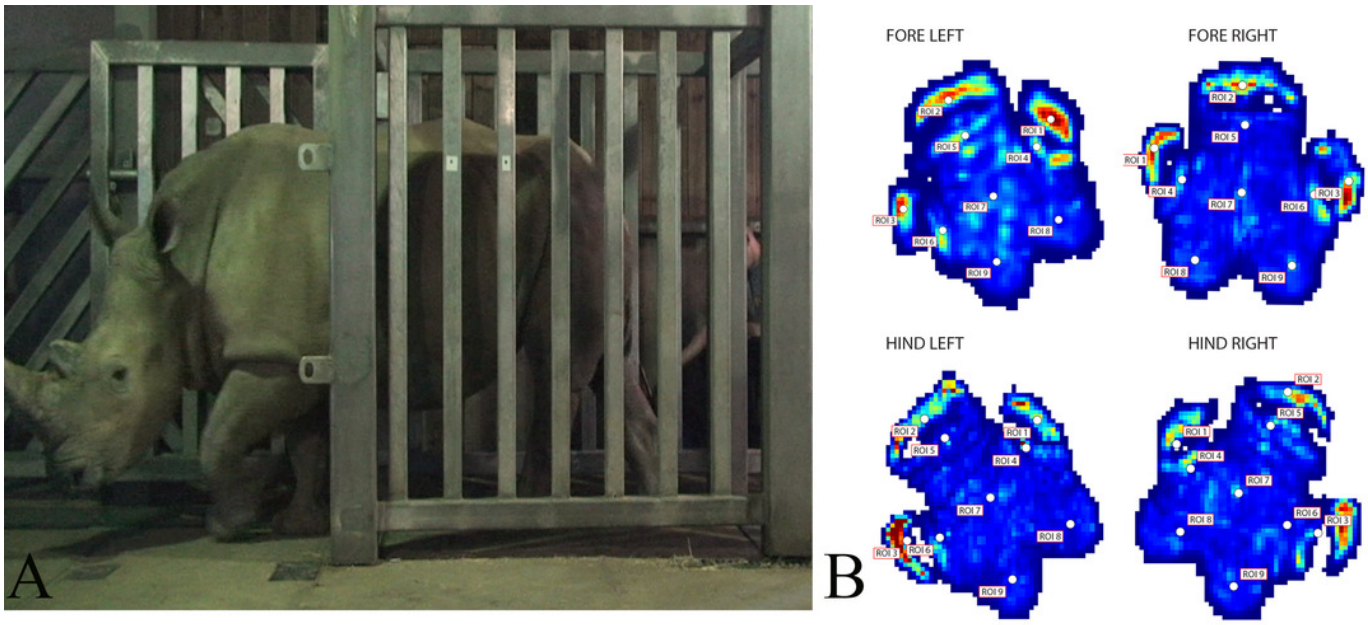

Figure 2(on next page)

Scatter plot of peak foot pressure data from all three subjects at the nine regions of interest (ROI) across the left forefoot, right forefoot, left hindfoot and right hindfoot respectively.

Black line represents the median pressure found at each ROI.

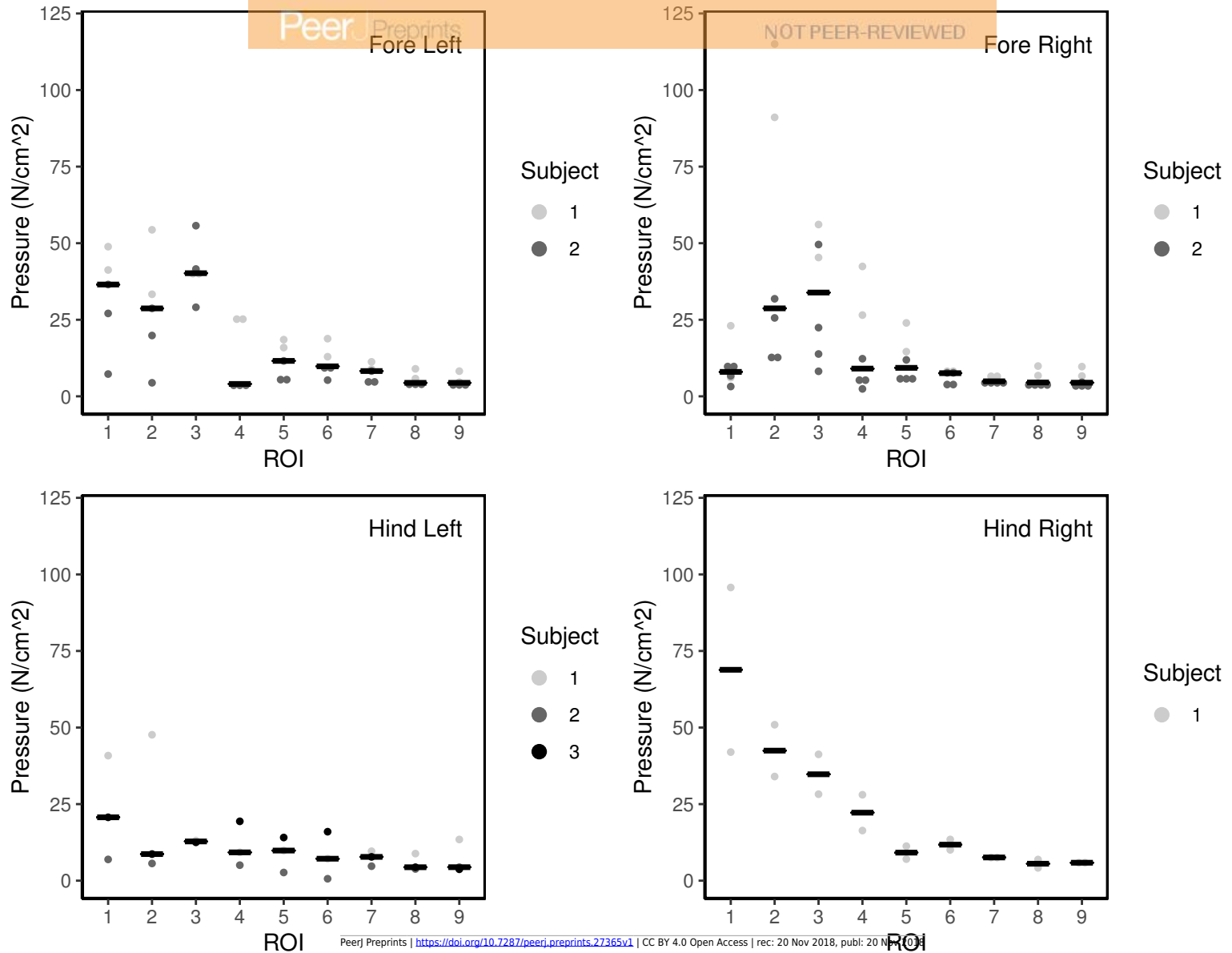

PeerJ Preprints | https://doi.org/10.7287/peerj.preprints.27365v1 | CC BY 4.0 Open Access | rec: 20 Nov 2018, publ: 20 Nov 2018

Figure 3

Peak pressure patterns during the whole stance phase of the left forefoot of all subjects.

Fore Left

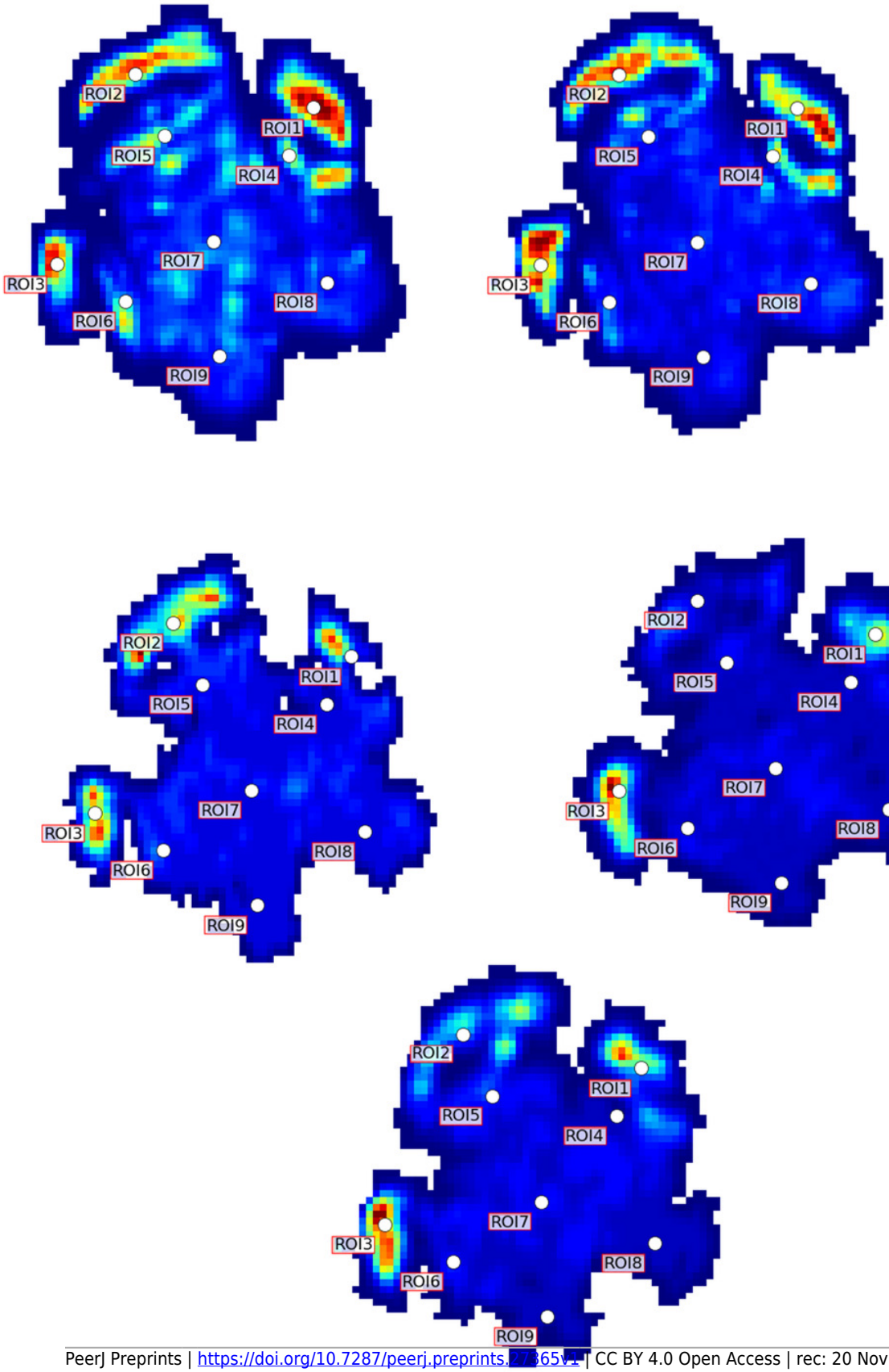

Figure 4

Peak pressure patterns during the whole stance phase of the right forefoot of all subjects.

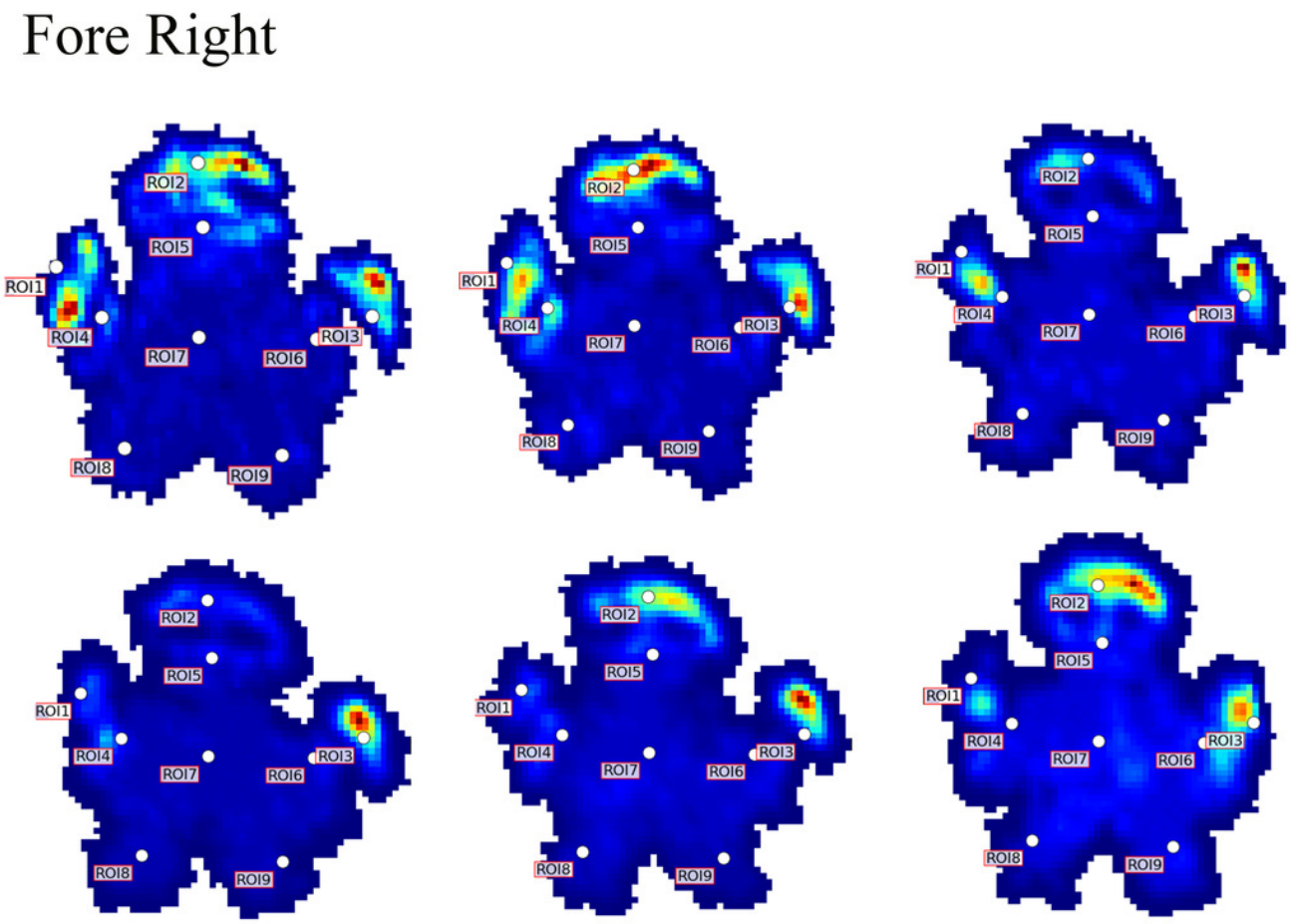

Figure 5

Peak pressure patterns during the whole stance phase of the left hindfoot of all subjects.

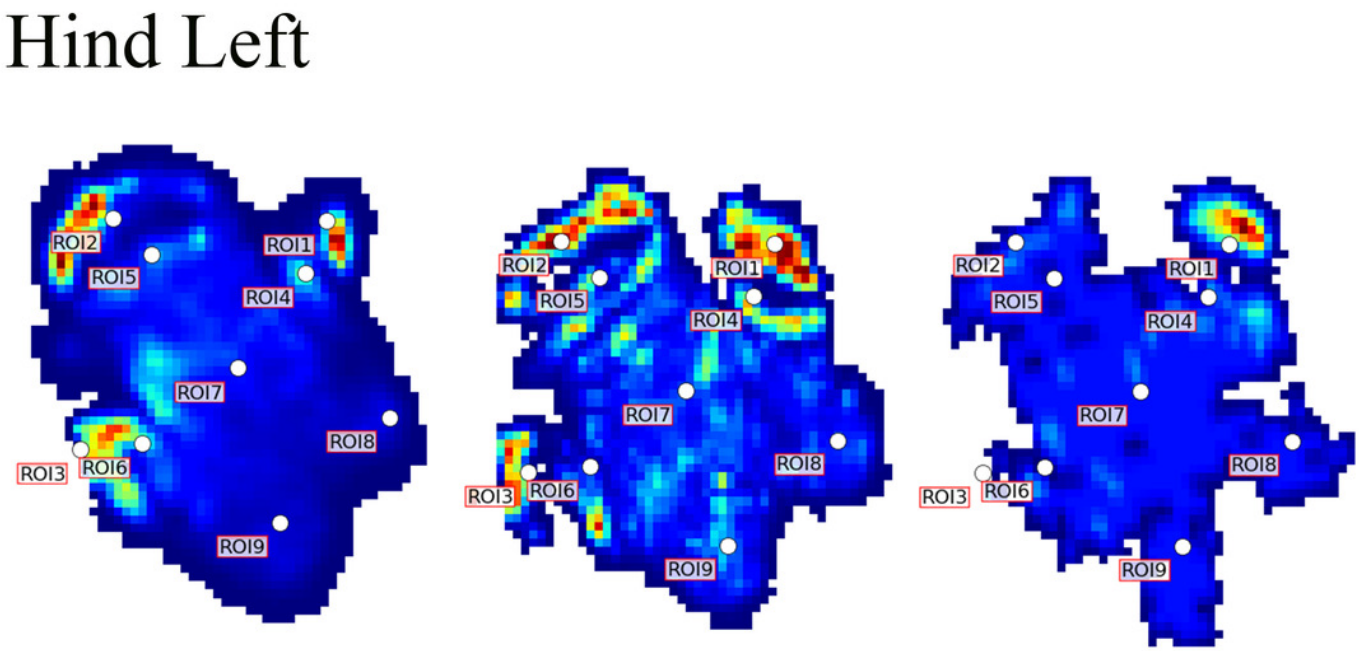

Figure 6

Peak pressure patterns during the whole stance phase of the right hindfoot of all subjects.

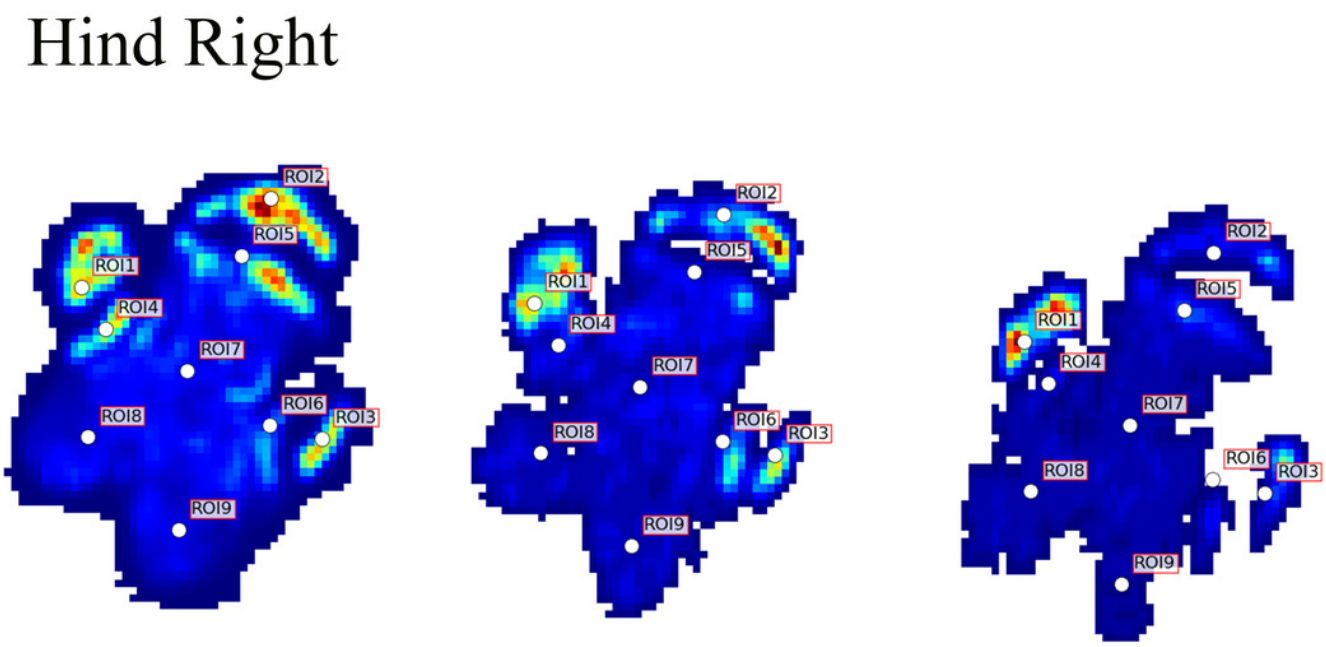

Table 1(on next page)

Subject characteristics (*Ceratotherium simum*).

Table 1. Subject characteristics (*Ceratotherium simum*).

	Subject 1	**Subject 2**	**Subject 3**
Age	Adult	Juvenile	Adult
Sex	Female	Female	Female
Body mass (kg)- estimated	2500	1000	2500
Shoulder height (m)	1.5	0.65	1.42
Mean Froude number	0.014	0.001	0.054
Mean velocity (ms^{-1})	0.46	0.60	0.87
Mean maximum pressure ($N\ cm^{-2}$) Fore Left 1	23	13	No spatially/temporally complete data
Mean maximum pressure ($N\ cm^{-2}$) Fore Right 2	28	9	No spatially/temporally complete data
Mean maximum pressure ($N\ cm^{-2}$) Hind Left 3	18	4	12
Mean maximum pressure ($N\ cm^{-2}$) Hind Right 4	2	No spatially/temporally complete data	No spatially/temporally complete data
Number of Steps	4	3	1